Drug Design, Development and Therapy

Dovepress
open access to scientific and medical research

Open Access Full Text Article

ORIGINAL RESEARCH

# Neohesperidin Ameliorates Steroid-Induced Osteonecrosis of the Femoral Head by Inhibiting the Histone Modification of lncRNA HOTAIR

This article was published in the following Dove Press journal:
*Drug Design, Development and Therapy*

Shuai Yuan*
Chuanxin Zhang*
Yunli Zhu
Bo Wang

Department of Joint Surgery and Sports Medicine, Changzheng Hospital, Naval Medical University, Shanghai, People's Republic of China

*These authors contributed equally to this work

**Background:** Neohesperidin (NH) and lncRNA HOTAIR (HOTAIR) could regulate osteoclastic and osteogenic differentiation. This study aimed to explore whether HOTAIR-mediated osteogenic differentiation was regulated by NH.

**Methods:** Steroid-induced osteonecrosis of the femoral head (SONFH) mice model was established. Histopathological changes in mouse osteonecrosis tissues were detected by hematoxylin-eosin staining. Bone marrow stromal cells (BMSCs) were isolated from healthy mice bone marrow samples by Ficoll density gradient and identified by flow cytometry. After treating the BMSCs with NH and dexamethasone or transfecting with HOTAIR overexpression plasmids and siHOTAIR, histone modification of HOTAIR, the cell viability, osteogenic differentiation, and adipogenic differentiation were detected by chromatin immunoprecipitation, MTT, Alizarin Red and Oil Red O staining, respectively. The expressions of HOTAIR and differentiation-related factors in the BMSCs were detected by RT-qPCR and Western blot.

**Results:** HOTAIR was highly expressed in SONFH model mice. NH ameliorated histopathological changes in the model mice, but the effect was reversed by overexpressed HOTAIR. NH increased viability of BMSCs and the H3K27me3 occupancy of HOTAIR, but decreased the expression and the H3K4me3 occupancy of HOTAIR. HOTAIR expression was down-regulated in BMSCs after osteogenic differentiation but was up-regulated after adipogenic differentiation. HOTAIR overexpression inhibited osteogenic differentiation and the expressions of RUNX2, OCN, and ALP, but increased adipogenic differentiation and the expressions of LPL and PPARr in BMSCs; moreover, the opposite results were observed in siHOTAIR.

**Conclusion:** NH ameliorated SONFH by inhibiting the histone modifications of HOTAIR.

**Keywords:** neohesperidin, HOTAIR, bone marrow stromal cells, osteogenesis, adipogenic

## Introduction

Osteonecrosis of the femoral head (ONFH) is a refractory disease, manifested by the death of osteocytes and bone marrow components, which is related to the internal structure changes of the femoral head and inevitably causes collapse.[1] There are about 500,000–7,500,000 ONFH patients in China.[2] The incidence of steroid-induced ONFH (SONFH) is a non-traumatic type of ONFH with the highest incidence,[3] and clinically, total hip replacement is the main treatment for SONFH.[4,5] SONFH is closely related to the defect of BMSCs, but the exact mechanism underlying SONFH development remains unclear.[6]

Correspondence: Bo Wang
Department of Joint Surgery and Sports Medicine, Changzheng Hospital, Naval Medical University, No. 415, Fengyang Road, Huangpu District, Shanghai 200003, People's Republic of China
Tel +86-21-81885639
Email wangbo_wbob@163.com

submit your manuscript | www.dovepress.com
DovePress
http://doi.org/10.2147/DDDT.S255276

BMSCs have a crucial effect on normal bone metabolism for their self-renewal ability and differentiation into osteoblasts, adipocytes, chondrocytes, and endothelial cells.[7–9] Therefore, BMSCs are regarded as ideal seed cells for the therapy of a series of human bone diseases.[10,11] In addition, declined functions of BMSCs, which were reported to be related to non-traumatic ONFH,[6] were also observed in SONFH patients.[12,13] On the basis of these findings, enhancing the differentiation of BMSCs may be a potential method for the treatment of SONFH.

Neohesperidin (NH), an extract from citrus fruits, is a flavanone glycoside with a strong bitter taste.[14] With numerous beneficial pharmacological properties, NH gradually became a new therapy to various disorders.[15] For instance, NH has been found to suppress the development of colorectal cancer through affecting intestinal flora;[15] NH exerts inhibitory effects on gram-negative and gram-positive bacteria[16] and HCl/ethanol-induced gastric lesions, therefore might be useful for the protection of gastritis;[17] also NH could inhibit osteoclast differentiation and bone resorption.[18] However, the effect of NH on the differentiation of BMSCs still remained unknown. HOTAIR, a well-characterized oncogenic lncRNA, has been proven to have inhibitory effects on osteogenic differentiation of BMSCs in non-traumatic osteonecrosis of femoral head,[19–21] but whether HOTAIR-mediated differentiation could be regulated by NH should be examined.

Based on the previous findings, we speculated that NH had an effect on the differentiation of BMSCs via regulating HOTAIR by conducting a series of experiments.

# Materials and Methods

## Ethics Statement

All animal experiments were performed in accordance with the guidelines of the Chinese Association for Laboratory Animal Sciences. This study was approved by the Ethical Committee of Experimental Animals of Shanghai Changzheng Hospital, Naval Medical University (Z20190432G). Every effort has been made to minimize pain and discomfort caused to the animals. The animals' experiments were performed in Shanghai Changzheng Hospital.

## Animal and SONFH Model Establishment

Seventy male healthy C57BL/6J mice (weight: 18.82 ±1.54 g, age: 6 weeks old) purchased from SLAC Laboratory Animal Technology Co. (Shanghai, China) to establish a SONFH model as described previously.[22] The mice were randomly divided into seven groups (n=10), namely, Control, Model, NH, NH+NC, NH+HOTAIR, NC and HOTAIR groups. For the Control group, normal saline (R21479, Yuanye, Shanghai, China) was subcutaneously injected into the right hind legs of each mouse twice a week for 6 weeks. For the Model group, methylprednisolone (20 mg/kg body weight) (M830013, Macklin, shanghai, China) was subcutaneously injected into one of the right hind legs of each mouse twice a week for 6 weeks. For NH group, on the basis of the Model group, the mice were further given a daily intragastric administration of NH (22.5 g/d/kg-bodyweight) (13,241–33-3, Yuanye) during the 6 weeks. For NH+NC group, on the basis of NH group, the mice were further injected with $3 \times 10^{12}$ negative control lentiviral (ENECHEM, Shanghai, China) via the same hind legs muscle once a week during the 6 weeks. For NH +HOTAIR group, on the basis of NH group, the mice were further injected with $3 \times 10^{12}$ HOTAIR overexpression lentiviral (ENECHEM, Shanghai, China) via the same hind leg muscle once a week during the 6 weeks. For NC group, on the basis of model group, the mice were further injected with $3 \times 10^{12}$ negative control lentiviral via the same hind leg muscle once a week during the 6 weeks. For HOTAIR group, on the basis of model group, the mice were further injected with $3 \times 10^{12}$ HOTAIR overexpression lentiviral via the same hind leg muscle once a week during the 6 weeks. All the mice were housed in cages together for 12 weeks (including 6 weeks after completing treatment) and provided with free access to food and water for the whole period. After 12 weeks of culture, the mice were sacrificed under general anesthesia with an overdose of pentobarbital (80 mg/kg) (B005, Beyotime, Shanghai, China). The right hind legs and the corresponding femoral tissues were harvested and dissected under sterile conditions.

## H&E Staining

The femoral tissues were collected and paraffin-embedded (S25190, Yuanye), fixed on a microtome (RM2235, Leica, Solms, Germany) and sliced into 8 μm thick. Then, the slices were fixed on a glass slide (80,302–3101-16-P4, ShiTai, Jiangsu, China) and deparaffinized. Next, the tissue slices were incubated with hematoxylin (B25380, Yuanye) for 10 mins and then with eosin (G1100, Solarbio, Beijing, China) for 1min at room temperature. Finally, indexes were detected using a phase-contrast

optical microscope (Magnification ×100 and ×200) (Axio Lab.A1 pol; Leica, Solms, Germany).

## Micro-CT

The Micro-CT (μCT, GE Healthcare Biosciences, Piscataway, USA) was used to detect the changes in the mouse femoral head and bone trabeculae tissues. The following parameters were calculated (Table 1): bone volume (BV)/tissue volume (TV), trabecular bone pattern factor (Tb.Pf), trabecular thickness (Tb.Th), trabecular number (Tb.N), trabecular separation (Tb.Sp), and bone mineral density (BMD).

## Isolation and Culture of BMSCs

Three male healthy C57BL/6J mice (weight: 18.82±1.54 g, age: 2–3 weeks old) purchased from SLAC Laboratory Animal Technology Co. (Shanghai, China) were used for obtaining BMSCs. The BMSCs were isolated from the femoral tissues of the healthy mice by Ficoll density gradient.[2,23] In brief, after the hind legs and the corresponding femoral tissues were harvested, the bone marrow samples were filtered through a 100 mm filter (251600506SC, Merck Millipore, Darmstadt, Germany) and further mixed with Hanks buffer (C0218, Beyotime), and then lymphoprep (07851, Stemcell, Canada) was gently layered. The samples were then centrifuged for 30 mins at 20 °C (400 × g), and the cells located at the interface between the bone marrow sample and lymphoprep were the BMSCs. The BMSCs were collected and further cultured in Dulbecco's modified Eagle's medium (DMEM) (C11995500BT, Gbico, MA, USA) containing 10% fetal bovine serum (FBS) (10,437,010, Gbico), 10 U/mL penicillin (DEPENE01, Demeditec, Germany), and 10 mg/mL streptomycin (DESTRE02, Germany) at 37°C in a humid atmosphere with 5% $CO_2$. For morphological observation, the cells were observed under a phase-contrast optical microscope (Magnification ×200) (Axio Lab.A1 pol, Leica, Solms, Germany), and flow cytometry was conducted for the identifying BMSCs.

After identification, the BMSCs were divided into three groups. In the first group, the BMSCs were cultured in DMEM complete medium and treated with 50 μmol/L NH alone for chromatin immunoprecipitation (ChIP) assay. In the second group, the BMSCs were cultured in DMEM complete medium and co-treated with NH and dexamethasone (DEX) (D829854, Macklin) for MTT assay and RT-qPCR. In the third group, the BMSCs were cultured in osteogenic medium (SH30881.02, Hyclone, Logan, USA) or adipogenic medium (SH30886.02, Hyclone) and transfected with HOTAIR overexpression plasmids and siHOTAIR for Alizarin Red staining and Oil Red O staining, Western blot, and RT-qPCR.

## Flow Cytometry

Flow cytometry was performed to identify the phenotype of the BMSCs isolated from bone marrow tissues. In brief, the cells were harvested and re-suspended in fluorescence-activated cell sorting (FACS) buffer (MB-089-0500, Dickinson Biosciences, Philadelphia, USA) and incubated with the primary unconjugated antibodies CD29 (MAB17781, R&D System, MA, USA), CD90 (ab133350, Abcam, CA, USA) and CD34 (ab81289, Abcam) for 25 mins at 20 °C. The cells were washed and then incubated with secondary antibody goat anti-mouse IgG (ab102291, Abcam) for 15 mins. Finally, the cells were identified by flow cytometry on a FACS Calibur (Becton Dickinson, Oxford, UK). The data were analyzed using FCS Express software 3.0 (Dickinson Biosciences).

## ChIP Assay

Cross-linking and ChIP were conducted as described previously[24] at 0–4 °C, and all the buffers were supplemented with 0.1 mM EDTA (15,576,028, Gibco), 0.5 mM EGTA (S30018, Yuanye), 1 mM dithiothreitol (15,508,013, Gibco), and protease inhibitors (27,588,800, Aks mics, Shanghai, China). After BMSCs were treated with 50 μmol/L NH, the BMSCs were washed with phosphate-buffered saline (PBS)

**Table 1** Parameters of Femoral Head and Bone Trabeculae in Mice

| | Control | Model | NH | NH+NC | NH+HOTAIR | NC | HOTAIR |
|---|---|---|---|---|---|---|---|
| BV/TV (%) | 80±11.3 | 30±3.9*** | 78±11.1$^{\wedge\wedge\wedge}$ | 80±11.4$^{\#\#\#}$ | 28±4.1$^{\&\&\&\Delta+++}$ | 33±4.8 | 20±3.0$^{\wedge}$ |
| Tb.Pf (1/mm) | 30±4.3 | 10±1.4*** | 31±4.2$^{\wedge\wedge\wedge}$ | 32±4.0$^{\#\#\#}$ | 11±1.5$^{\&\&\&+++}$ | 12±1.6 | 8±1.2 |
| Tb.Th (mm) | 0.25±0.04 | 0.05±0.01*** | 0.22±0.04$^{\wedge\wedge\wedge}$ | 0.23±0.04$^{\#\#\#}$ | 0.04±0.01$^{\&\&\&+++}$ | 0.05±0.01 | 0.03±0.01 |
| Tb.N (1/mm) | 10±1.4 | 5±0.7*** | 9±1.3$^{\wedge\wedge\wedge}$ | 8.8±1.2$^{\#\#\#}$ | 4.8±0.7$^{\&\&\&\Delta+++}$ | 5.1±0.7 | 3±0.4$^{\wedge}$ |
| Tb.Sp (mm) | 0.04±0.01 | 0.12±0.02*** | 0.04±0.01$^{\wedge\wedge\wedge}$ | 0.04±0.01$^{\#\#\#}$ | 0.15±0.03$^{\&\&\&\Delta+++}$ | 0.13±0.02 | 0.2±0.03$^{\wedge\wedge}$ |
| BMD (g/mm$^3$) | 700±98 | 200±29*** | 650±92$^{\wedge\wedge\wedge}$ | 648±93$^{\#\#\#}$ | 190±27$^{\&\&\&\Delta+++}$ | 202±30 | 150±21$^{\wedge\wedge}$ |

**Notes:** ***$P$ <0.001 vs Control; $^{\wedge}P$ <0.05; $^{\wedge\wedge}P$ <0.01; $^{\wedge\wedge\wedge}P$ <0.001 vs Model; $^{\#\#\#}P$ <0.001 vs NC; $^{\&\&\&}P$ <0.001 vs NH; $^{\Delta}P$ <0.05 vs HOTAIR; $^{+++}P$ <0.001 vs NH+NC.

(C0221A, Beyotime) and lysed. After centrifugation, the pellet was re-suspended in 10 mL of 10 mM pH 8.0 Tris-HCl (10,812,846,001, ROCHE, Barcelona, Switzerland) and 200 mM NaCl (A610476-0005, Sangon Biotech, Shanghai, China), rotated for 10 mins and further centrifuged at 15,000 ×g for 10 mins. The chromatin pellet was re-suspended in 1 mL of 50 mM pH 7.9 Tris-HCl and 5 mM $CaCl_2$ (20–305, Merck Millipore) and digested with 500 units of micrococcal nuclease (LN101-02, TransGen Biotech, Shanghai, China) at 37 °C for 10 mins. For ChIP reactions, the samples (1 mL) were incubated with anti-H3K4me3 (ab8580, Abcam), anti-H3K27me3 (ab6002, Abcam), or control rabbit IgG (ab172730, Abcam) overnight before the IP. Finally, 3 μL ChIP DNA was purified and quantified using RT-qPCR.

## MTT Assays

MTT (B7777, APExBIO, Houston, USA) was performed to determine the cell viability. The BMSCs were cultured with 1 μmol/L DEX alone for 1 hr or co-treated DEX with NH (12.5 μmol/L, 25 μmol/L, or 50 μmol/L) and further cultured for different times (1–3 days) at 37°C in a humid atmosphere with 5% $CO_2$, then the cells were laid into 96-well plates containing 100 μL complete medium at $1.0 \times 10^4$ cells. After growing for 1–3 days, the cells were incubated with MTT reagent (0.5 mg/mL) for 4 hrs. Then, the MTT solution was discarded and 100 μL DMSO (ST038, Beyotime) was added into each well. Finally, the absorbance of each well was read at 570 nm by a microplate reader (Infinite M200 PRO, Tecan Austria GmbH, Austria).

## Transfection

Plasmids overexpressing HOTAIR ligated into pcDNA3.1 (lnc4000273-1-2), negative control for overexpression HOTAIR (NC; lnc6N0000002-1-10), siHOTAIR (siHOTAIR; lnc3151124051110), and negative control for siHOTAIR (siNC; lnc3N0000001-1-5) were obtained from RIBOBIO (Guangzhou, China). RNase-free $H_2O$ (ST876, Beyotime) was used to dilute these products and stored at −20°C for later use. Before transfection, the BMSCs at $1.0 \times 10^6$ cells were plated into 6-well plates containing 2 mL osteogenic or adipogenic medium. After growing overnight until the cell confluence reached 20%-30%, 100 μL osteogenic or adipogenic medium was used to dilute 2 μg plasmids and siHOTAIR. Three microliters lipofectamine 2000 (11,668–019, Invitrogen, MA, USA) was added into 100 μL osteogenic or adipogenic medium, and then the two media were mixed together and incubated for 15 mins at room temperature. Finally, the mixed liquid was added into the cells of each well, and further added with 1.8 mL osteogenic or adipogenic medium for an additional 48 hrs.

## Alizarin Red Staining

The staining was conducted using an Alizarin Red S staining kit (0223, ScienCell, CA, USA). After the BMSCs were transfected with plasmids and siHOTAIR and further cultured in osteogenic medium for 12 days, the BMSCs were collected and washed with PBS twice. Then, the cells were fixed with 97% ethanol (E111992-12X, Aladdin, Shanghai, China) for 10 mins. Finally, the fixed cells were incubated with Alizarin Red staining solution for 30 mins at 37 °C and observed under a phase-contrast optical microscope (Magnification ×100) (Axio Lab.A1 pol, Leica, Solms, Germany).

## Oil Red O Staining

After the BMSCs were transfected with plasmids and siHOTAIR and further cultured in adipogenic medium for 20 days, the BMSCs were collected and washed with PBS and further incubated with Oil Red O (ab146295, Abcam) at 25 °C for 30 mins. Next, the cells were washed with 75% ethanol (80,176,961, HUSHI, Beijing, China) and washed with PBS. Finally, the cells were observed under a phase-contrast optical microscope (Magnification ×200) (Axio Lab.A1 pol; Leica, Solms, Germany).

## RNA Extraction and RT-qPCR

Total RNAs were extracted from the femoral tissues and BMSCs using TRIzol reagent (15,596, Invitrogen, MA, USA) following the instructions. Briefly, the tissues and cells were lysed by TRIzol and collected into a new 1.5 mL centrifugal tube (615,001, Nest, Wuxi, China), added with chloroform (C805334, Macklin) and centrifuged for 20 mins (14,000 × g). The supernatant was collected and added with an equal volume of isopropanol (H822173, Macklin), and centrifuged for 5 mins (14,000 × g). RNA sediment was diluted using RNase-free $H_2O$. Then, PrimeScript RT kit (RR037A, Takara, Dalian, China) was used to reverse-transcribe RNA into cDNA according to the reference instructions. Finally, gene expression was determined by RT-qPCR assays using Verso 1-step RT-qPCR Kit (A15300; Thermo Scientific, MA, USA) in ABI 7500 Fast Real-Time PCR System (Applied Biosystems, CA, USA) under the following conditions of RT-qPCR: at 95°C for 30 s, 60°C for 30 s, 45 cycles at 60°C for 30 s. RNA

expressions were quantified by $2^{-\Delta\Delta CT}$ method.[25] All the primer sequences are shown in Table 2.

## Western Blot

Total protein from the BMSCs transfected with plasmids and siHOTAIR was isolated by RIPA lysis buffer (P0013B, Beyotime), and a BCA assay kit (23,250, Pierce, MA, USA) was used to detect the total protein concentrations. The total protein (30 μg) was separated in each lane on 10% SDS-PAGE gels (P0052A, Beyotime), electro-blotted and transferred to NC membranes (HTS112M, Millipore). Then, all the membranes were incubated by 5% skimmed milk for 2 hrs at normal atmospheric temperature, and followed by incubation with relative primary antibodies as follows: ALP (1:1000, 39kD, ab83259, Abcam), OCN (1:1000, 12kD, ab93876, Abcam), RUNX2 (1:1000, 37kD, ab76956, Abcam), LPL (1:1000, 25kD, ab91606, Abcam), PPARr (1:1000, 57kD, ab45036, Abcam), and GAPDH (1:1000, 37kD, ab181602, Abcam). The next day, HRP-conjugated goat anti-rabbit IgG secondary antibody (1:5000, ab205718, Abcam) or goat anti-mouse IgG secondary antibody (1:5000, ab205719, Abcam) was incubated with the membranes for 1 hr at room temperature. Finally, the membranes were incubated with SuperSignal West Pico Chemiluminescent Substrate (34,078, Thermo Scientific, MA, USA) for signal detection. Image Lab™ Software (version 3.0) was used for densitometric analysis and quantification of the Western blot data (Bio-Rad Laboratories Inc., Hercules, CA, USA).

## Statistical Analysis

Student's *t*-test and one-way ANOVA were applied to analyze the data generated in this study using SPSS software (version 18.0). LSD and Dunnet's were post hoc tests. The statistical data were presented as Mean ± standard deviation. All the experiments were conducted three times. Statistically significant was defined as $P < 0.05$.

# Results

## NH Reduced Histopathological Changes and HOTAIR Expression in the Mice with SONFH

A comparative analysis of HOTAIR expression among the Model, NH, and NH+HOTAIR groups was conducted on the femoral tissues collected (Figure 1A). The result revealed that HOTAIR expression was obviously up-regulated in Model group compared with that in Control group ($P < 0.001$), while the HOTAIR expression was obviously down-regulated by NH treatment as compared with that in Model group ($P < 0.001$). Additionally, overexpression of HOTAIR reversed the effects of NH ($P < 0.001$). H&E staining was performed to observe the pathological changes of the tissues, as shown in Figure 1B, expansion of typical cavity necrosis areas and increase of bone marrow cell debris appeared in the Model group, but NH treatment significantly reduced such changes in the Model group. Additionally, overexpression of HOTAIR reversed the effects of NH. The changes in the femoral head tissues and bone trabeculae were further examined by a Micro-CT. As shown in Table 1, the BV/TV, Tb.Pf, Tb.Th, and Tb.N were significantly reduced, and the Tb.Sp was greatly increased in the Model group as compared with Control group ($P < 0.001$). NH treatment alleviated steroid-induced changes of these parameters in the mice. In addition, overexpression of HOTAIR reversed the effect of NH on these microstructural parameters. Moreover, BMD value was also measured to determine whether NH treatment increased bone mass of the SONFH mice. As shown in Table 1, the SONFH mice (Model group) showed markedly reduced BMD value as compared with the Control group ($P < 0.001$). The BMD value in the NH group was increased as compared with that in Model group ($P < 0.001$), whereas

**Table 2** RT-qPCR Primers

| Target Gene | Forward Primers, 5′–3′ | Reverse Primers, 5′–3′ |
|---|---|---|
| *LncHOTAIR* | GGTAGAAAAAGCAACCACGAAGC | ACATAAACCTCTGTCTGTGAGTGCC |
| *RUNX2* | TGGTTACTGTCATGGCGGGTA | TCTCAGATCGTTGAACCTTGCTA |
| *OCN* | CTGACCTCACAGATCCCAAGC | TGGTCTGATAGCTCGTCACAAG |
| *ALP* | GAGATGTTGTCCTGACACTTGTG | AGGCTTCCTCCTTGTTGGGT |
| *LPL* | TTGCCCTAAGGACCCCTGAA | TTGAAGTGGCAGTTAGACACAG |
| *PPARr* | AACATCGAGTGTCGAATATGTGG | CCGAATAGTTCGCCGAAAGAA |
| *GAPDH* | AGGTCGGTGTGAACGGATTTG | GGGGTCGTTGATGGCAACA |

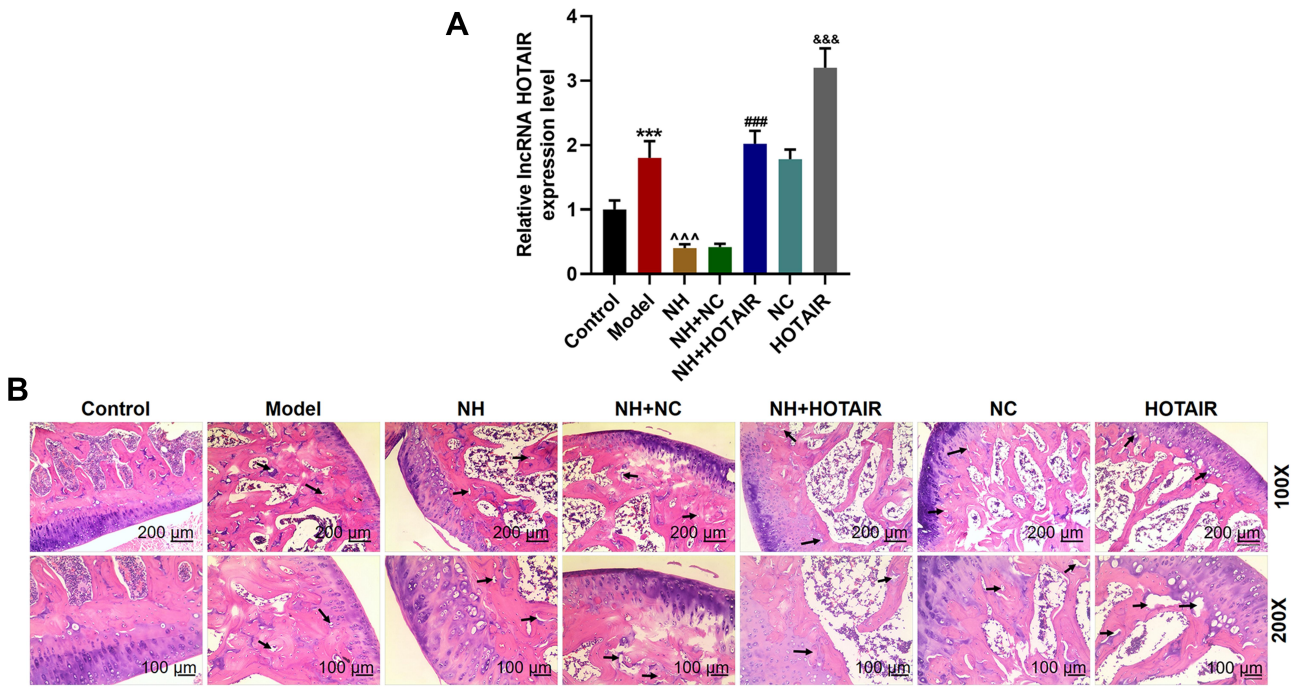


**Figure 1** NH reduced histopathological changes and decreased HOTAIR expression in the mice with SONFH, but HOTAIR overexpression reversed the effect of NH. (**A**) HOTAIR expression in the femoral tissues of the mice with SONFH was determined by RT-qPCR. GAPDH was an internal control. (***$P < 0.001$, vs Control; ^^^$P < 0.001$, vs Model; ###$P < 0.001$, vs NH+NC; &&&$P < 0.001$, vs NC). (**B**) H&E staining was conducted to observe the histopathological changes of femoral tissues (Magnification ×100 and ×200). All the experiments were conducted in triplicate.

**Abbreviations:** NH, Neohesperidin; SONFH, steroid-induced osteonecrosis of the femoral head; HE, Hematoxylin-eosin.

overexpression of HOTAIR reversed the effect of NH on the BMD value. These results revealed that NH treatment reduced histopathological changes and the expression of HOTAIR in the SONFH mice, suggesting that HOTAIR might play an important role in the occurrence or development of SONFH.

## BMSCs Were Isolated and Identified

In order to further investigate the effects of NH on SONFH and HOTAIR, the BMSCs were isolated from the normal femoral tissues derived from the healthy mice, further cultured and passaged. On day 7 of culture, primary cells were attached to the wall and exhibited spindle shapes; on day 3 of culture, passage 2 cells reached 90% confluence resembling a shoal of fish (Figure 2A). These characteristics were similar to those of BMSCs.[2,26] Then, phenotypes of passage 2 cells were identified by flow cytometry (Figure 2B), which demonstrated that 93.64% of the cells were CD29-positive and 98.55% of cells were CD90-positive, whereas 0.82% of the cells were CD34-negative. Therefore, most of the isolated cells expressed standard markers of BMSCs.

## NH Decreased Viability of DEX-Treated BMSCs and Expression of HOTAIR via Inhibiting the Histone Modifications of HOTAIR

As the histone methylations are associated with target gene expression in stem cells to regulate cell fate,[27] we then detected the effect of NH on the H3K4me3 (activating histone modification) and H3K27me3 (inhibiting histone modification) occupancies in the promoter of HOTAIR. As shown in Figure 3A, the ChIP assay exhibited that NH at 50 μmol/L decreased the occupancies of H3K4me3 but increased the occupancies of H3K27me3 as compared with control group ($P < 0.001$), indicating that NH could inhibit the histone modifications of HOTAIR in BMSCs. Mechanistically, we detected the effect of NH on the viability of BMSCs treated with DEX. As shown in Figure 3B, DEX significantly inhibited the viability of BMSCs as compared with control group ($P < 0.01$), while after co-treated with NH, 25 μmol/L and 50 μmol/L of NH remarkably increased the cell viability which inhibited by DEX as compared with DEX group ($P < 0.05$, $P < 0.01$, respectively). In addition, we further

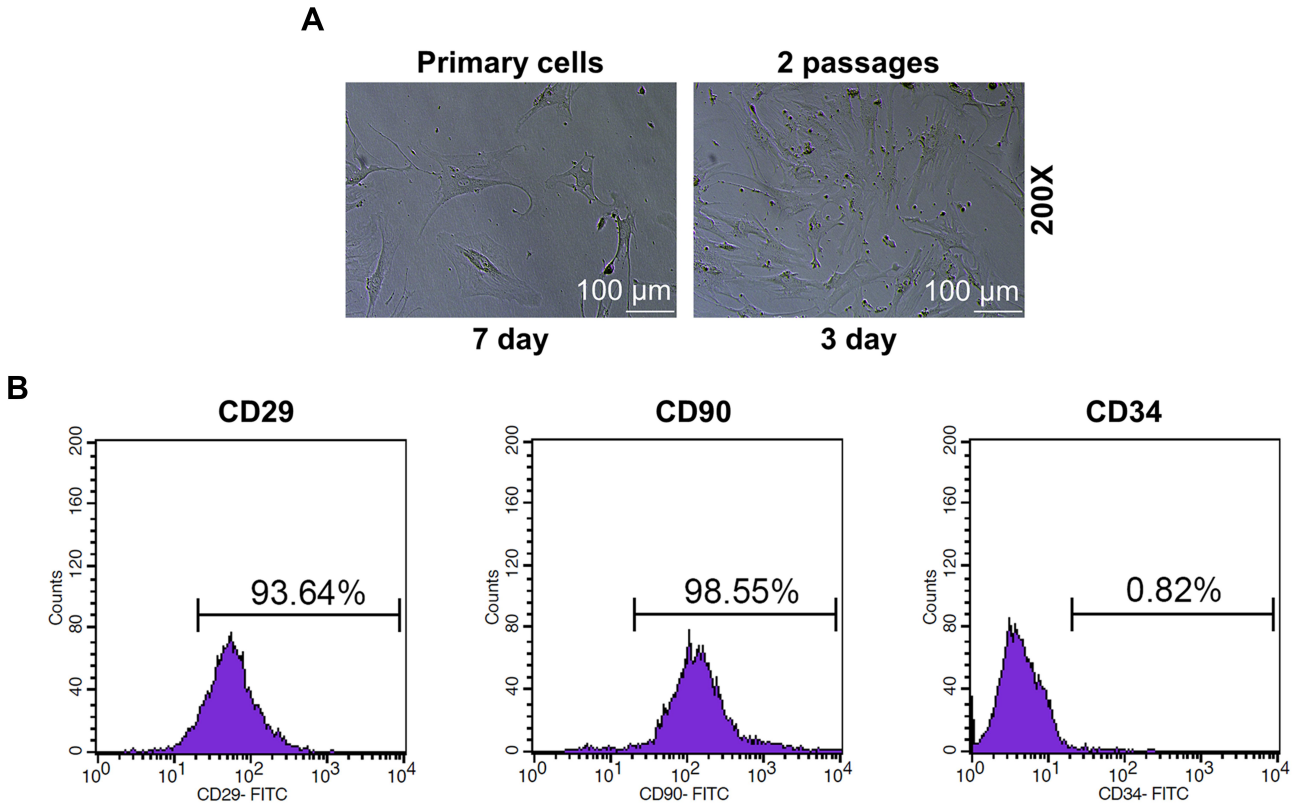


**Figure 2** BMSCs were isolated and identified. (**A**) Cell morphology of primary and BMSCs of passage 2 (Magnification ×200). (**B**) The expressions of the biomarkers in BMSCs were detected by flow cytometry. All the experiments were conducted in triplicate.
**Abbreviations:** NH, Neohesperidin; BMSCs, bone marrow mesenchymal stem cells.

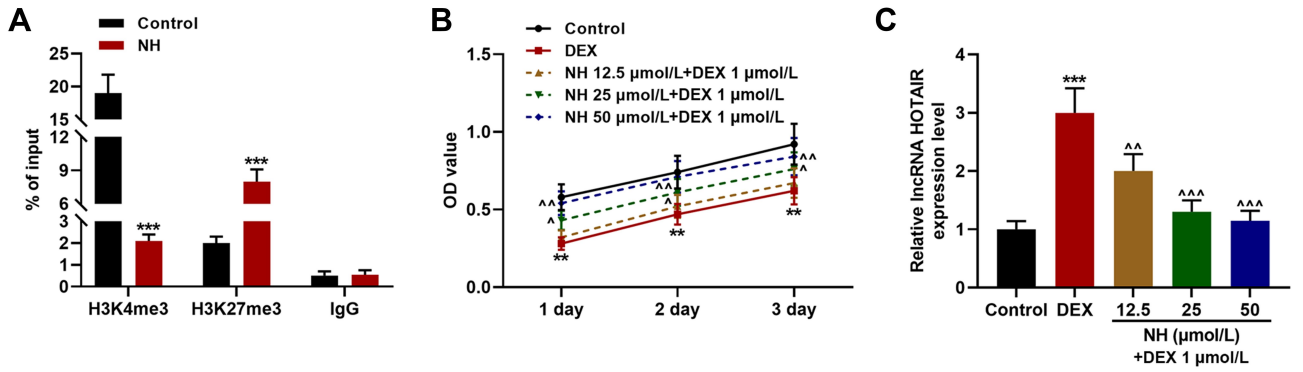


**Figure 3** NH reduced the viability of DEX-treated BMSCs and the expression of HOTAIR via inhibiting the histone modifications of HOTAIR. (**A**) The occupancies of H3K4me3 and H3K27me3 of SNHG1 promoter in the BMSCs after treated with NH were detected by ChIP assay. (**B**) The viability of BMSCs after treatment with DEX or NH was detected by MTT assays. (**C**) The expression of HOTAIR in BMSCs after treatment with DEX or NH was detected by RT-qPCR. GAPDH was an internal control. All the experiments were conducted in triplicate. (**$P < 0.01$, ***$P < 0.001$, vs Control; ^$P < 0.05$, ^^$P < 0.01$, ^^^$P < 0.001$, vs DEX).
**Abbreviations:** NH, Neohesperidin; DEX, dexamethasone; BMSCs, bone marrow mesenchymal stem cells; ChIP, chromatin immunoprecipitation.

detected the effect of NH on HOTAIR expression in BMSCs treated with DEX. As shown in Figure 3C, DEX significantly up-regulated HOTAIR expression as compared with control group ($P < 0.001$), while after co-treated with different doses of NH, NH remarkably decreased HOTAIR expression which inhibited by DEX as compared with DEX group ($P < 0.01$ or $P < 0.001$, respectively). All these results indicated that NH decreased the viability of DEX-treated BMSCs and HOTAIR expression via inhibiting the histone modifications of HOTAIR.

## Osteogenic Differentiation in BMSCs Was Inhibited by Overexpression of HOTAIR and Enhanced by siHOTAIR

To determine whether HOTAIR affects the behavior of BMSCs, the time-dependent expression pattern of HOTAIR during differentiation was analyzed. As shown in Figure 4A, HOTAIR expression was significantly decreased during osteogenic differentiation ($P < 0.01$ or $P < 0.001$) and increased during adipogenic differentiation ($P < 0.01$ or $P < 0.001$). Next, overexpressing HOTAIR plasmids or siHOTAIR was transfected into the BMSCs and RT-qPCR was used to detect the transfection efficiency (Figure 4B). Then, Alizarin Red staining was performed (Figure 4C), and the results showed that overexpression of HOTAIR significantly inhibited the osteogenic differentiation of BMSCs, evidenced by the decreased formation of calcium nodules of BMSCs after 12 days of culture in osteogenic medium, while siHOTAIR remarkably enhanced the osteogenic differentiation in BMSCs. Based on the current findings, we further detected the expressions of osteogenic marker genes (*ALP*, *OCN*, and *Runx2*) in BMSCs both at gene and protein levels. As shown in Figure 4D and E, overexpression of HOTAIR significantly reduced the expressions of *ALP*, *OCN*, and *Runx2* in the BMSCs as compared with NC group ($P < 0.001$), while siHOTAIR increased the expressions of *ALP*, *OCN*, and *Runx2* in BMSCs as compared with siNC group ($P < 0.01$). All these results revealed that osteogenic differentiation of BMSCs could be inhibited by overexpression of HOTAIR and enhanced by siHOTAIR.

## Adipogenic Differentiation in BMSCs Was Enhanced by Overexpression of HOTAIR and Inhibited by siHOTAIR

Furthermore, we also detected the effect of HOTAIR on adipogenic differentiation of the BMSCs. As shown in Figure 5A, Oil Red O staining results showed that overexpression of HOTAIR significantly enhanced the adipogenic differentiation of the BMSCs, which was supported by the increased formation of lipid droplets of BMSCs after 20 days of culture in adipogenic medium, but siHOTAIR remarkably inhibited the adipogenic differentiation of BMSCs. Based on these findings, we further detected the expressions of adipogenic marker genes (*LPL* and *PPARr*) in BMSCs both gene and protein levels. It can be observed from Figure 5B and C, overexpression of HOTAIR significantly increased the expressions of *LPL* and *PPARr* in BMSCs as compared with NC group ($P < 0.001$), while siHOTAIR decreased the expressions of *LPL* and *PPARr* in BMSCs as compared with siNC group ($P < 0.001$). Thus, all these results revealed that adipogenic differentiation of BMSCs could be enhanced by overexpression of HOTAIR and inhibited by siHOTAIR.

# Discussion

The progression of ONFH is closely related to decreased proportion of BMSCs and the abilities to proliferate and differentiate.[13] SONFH osteopathy lesion areas can exhibit excessive accumulation of fat and necrotic empty lacunae, at the same time accompanied by decreased expressions of osteogenic markers.[28,29] In this study, we also found the necrotic zone in the SONFH model mice showed a typical sign of empty lacunae. Changes in the characteristics of BMSCs' cells lead to the destruction of bone tissue, especially the differentiation of BMSCs.[30] Therefore, promoting the differentiation abilities of BMSCs may be a promising method for treating SONFH. A recent systematic review showed that Chinese herbal medicine as an adjuvant therapy could improve the condition of SONFH.[31]

NH, which is a natural flavanone glycoside with numerous pharmacological properties, has been widely used as herbal medicine in China.[14,15] In addition to the effects of anti-inflammation, neuro-protection, and cardiovascular protection, NH has also been reported to inhibit osteoclast differentiation.[18,32] In this study, we first found that NH could ameliorate histopathological changes in the SONFH mice. We further investigated the effects of NH on SONFH in vitro. Therefore, DEX was used to treat BMSCs to mimic under the condition of SONFH. After treating the BMSCs, we observed that NH significantly increased the cell viability previously decreased by DEX, suggesting that NH had a protective effect on SONFH, which further encouraged us to explore the underlying mechanism.

The changes of cell characteristics can be caused by abnormal gene expressions, non-coding RNAs, especially mRNAs, could regulate behaviors of BMSCs.[33–35] LncRNAs were widely investigated for their regulation of orthopedic disorders such as osteoarthritis and osteoporosis.[21,36] However, limited attention has been paid to the effect of lncRNAs on SONFH in the studies of lncRNAs. HOTAIR inhibits osteogenic differentiation of BMSCs, and is high-expressed in SONFH tissues.[21] Similarly, we also found that HOTAIR expression was highly expressed in osteonecrosis tissues of the SONFH

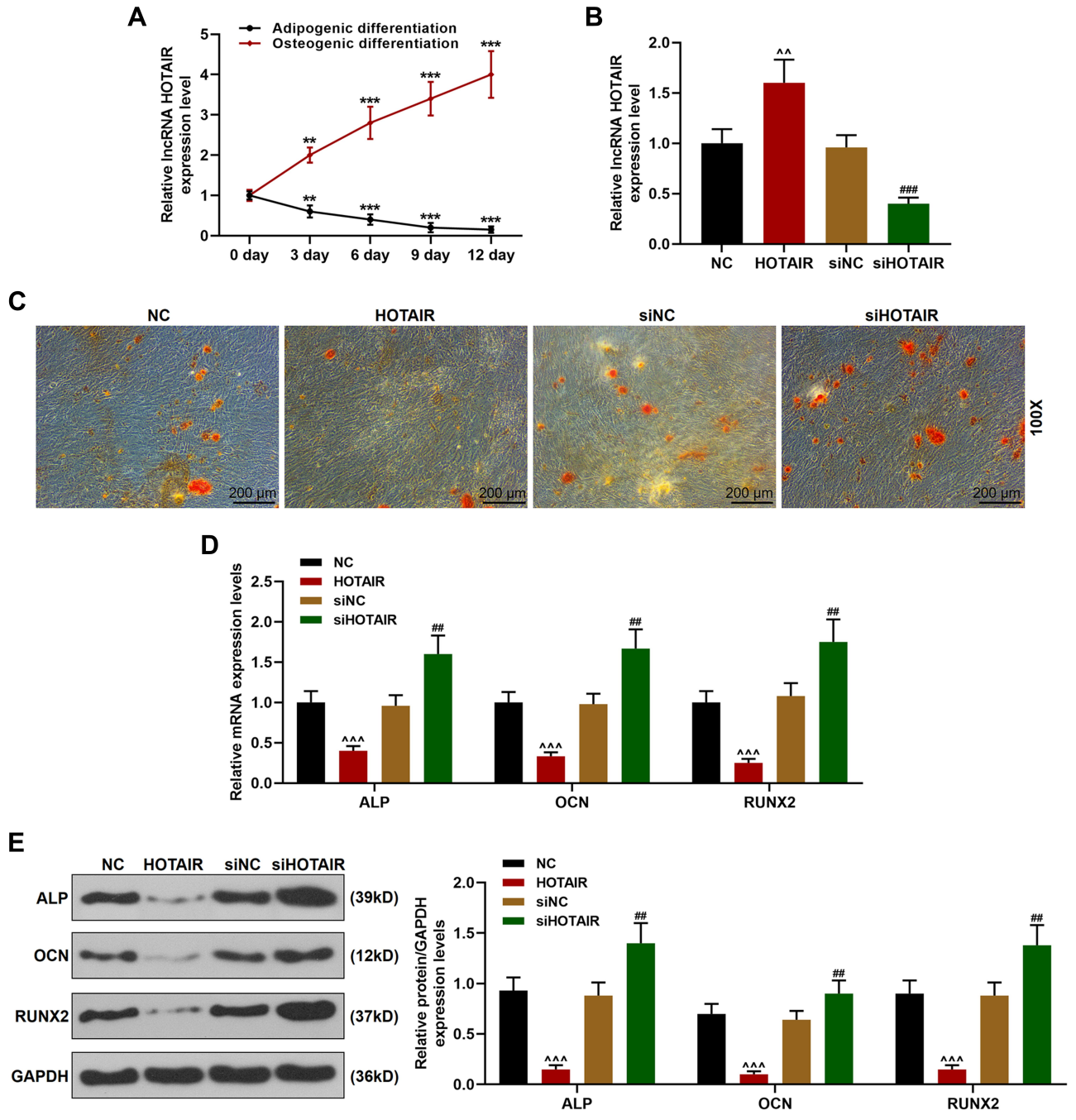


**Figure 4** Osteogenic differentiation of BMSCs was inhibited by overexpression of HOTAIR and enhanced by siHOTAIR. (**A**) The expression of HOTAIR in BMSCs after being cultured in osteogenic medium or adipogenic medium was detected by RT-qPCR. GAPDH was an internal control. (***P* < 0.01, ****P* < 0.001, vs 0 day). (**B**) Transfection efficiency of overexpressing HOTAIR plasmids and siHOTAIR was detected by RT-qPCR. GAPDH was an internal control. (**C**) The formation of calcium nodules in BMSCs after transfection was detected by Alizarin Red staining (Magnification ×100). (**D**) The expressions of *ALP*, *Runx2*, and *OCN* in BMSCs after the transfection were detected by RT-qPCR. GAPDH was an internal control. (**E**) The expressions of ALP, Runx2, and OCN in BMSCs after transfection was detected by Western blot. GAPDH was an internal control. All the experiments were conducted in triplicate. ($^{\wedge\wedge}P$ < 0.01, $^{\wedge\wedge\wedge}P$ < 0.001, vs NC; $^{\#\#}P$ < 0.01, $^{\#\#\#}P$ < 0.001, vs siNC).
**Abbreviations:** NH, Neohesperidin; BMSCs, bone marrow mesenchymal stem cells.

model mice. Therefore, we speculated that the protective effect of NH on SONFH was mediated through regulating HOTAIR expression. The results demonstrated that NH not only decreased the expression of HOTAIR in BMSCs but also inhibited the histone modifications of HOTAIR. In patients with bone diseases, the proportion of adipocytes is often increased concomitant with a decrease of BMSCs that could differentiate into osteoblasts.[37,38] Studies increasingly demonstrated the involvement of lncRNAs in osteogenic and adipogenic differentiation of BMSCs. Shuai

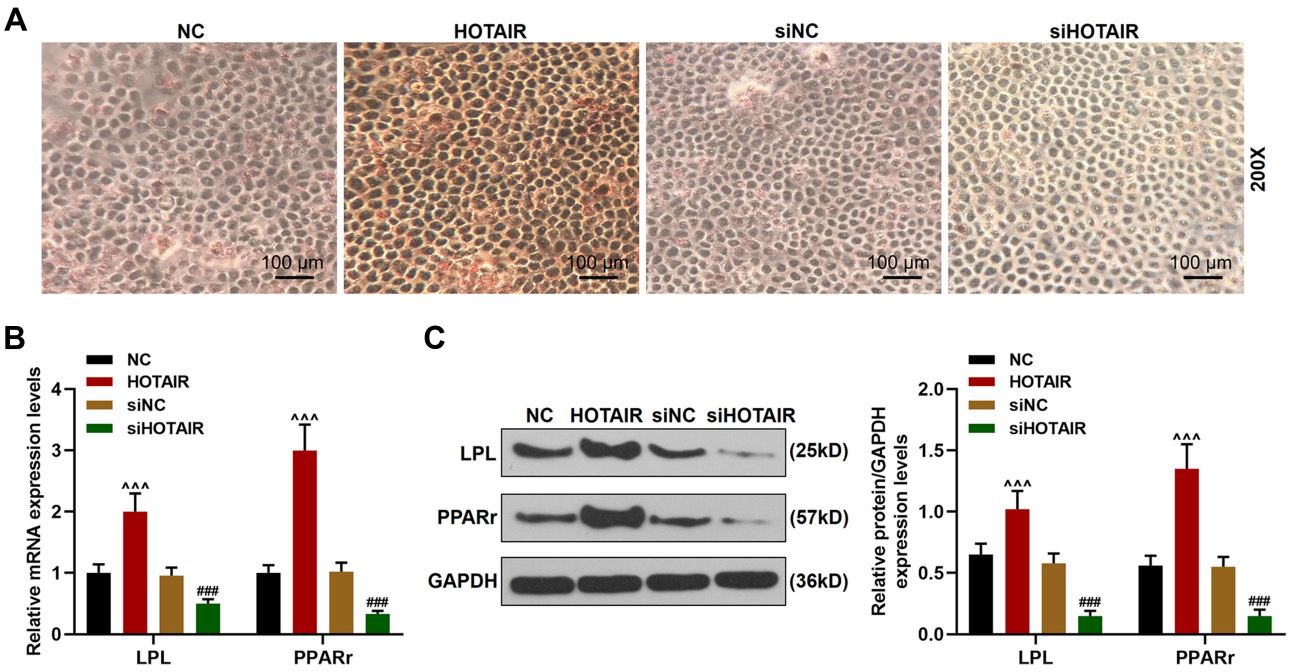


**Figure 5** Adipogenic differentiation in BMSCs was enhanced by overexpression of HOTAIR and inhibited by siHOTAIR. (**A**) The formation of lipid droplets in BMSCs after transfection was detected by Oil Red O staining (Magnification ×200). (**B**) The expressions of *LPL* and *PPARr* in BMSCs after transfection were detected by RT-qPCR. GAPDH was an internal control. (**C**) The expressions of LPL and PPARr in BMSCs after transfection were detected by Western blot. GAPDH was an internal control. All experiments were conducted in triplicate. ($^{\wedge\wedge\wedge}P < 0.001$, vs NC; $^{\#\#\#}P < 0.001$, vs siNC).
**Abbreviations:** NH, Neohesperidin; BMSCs, bone marrow mesenchymal stem cells.

et al reported that lncRNA RP11-154D6 promotes osteogenic differentiation and inhibits adipogenic differentiation of BMSCs;[39] lncRNA MEG3 inhibits adipogenic differentiation of adipose-derived MSCs.[40] In this study, we found the expression of HOTAIR was down-regulated during osteogenic differentiation but was up-regulated during adipogenic differentiation of BMSCs, indicating that HOTAIR might regulate the SONFH by mediating the differentiation of BMSCs. Subsequently, we found that overexpression of HOTAIR in BMSCs could inhibit trans-differentiation in the osteogenic direction and enhance trans-differentiation in the adipogenesis directions. These results demonstrated that overexpression of HOTAIR might promote lipid accumulation and reduce the repair of bone defects, thus contributing to the progression of SONFH.

## Conclusions

Based on current findings in this study, we could conclude that NH ameliorates SONFH by inhibiting the histone modifications of lncRNA HOTAIR.

## Data Sharing Statement

The analyzed data sets generated during the study are available from the corresponding author on reasonable request.

## Ethics Approval

All animal experiments were performed in accordance with the guidelines of the Chinese Association for Laboratory Animal Sciences. This study was approved by the Ethical Committee of Experimental Animals of Shanghai Changzheng Hospital, Naval Medical University (Z20190432G).

## Author Contributions

All authors made a significant contribution to the work reported, whether that is in the conception, study design, execution, acquisition of data, analysis and interpretation, or in all these areas.

All authors have drafted or written, or substantially revised or critically reviewed the article. All authors have agreed on the journal to which the article will be submitted. All authors reviewed and agreed on all versions of the article before submission, during revision, the final version accepted for publication, and any significant changes introduced at the proofing stage. All authors agree to take responsibility and be accountable for the contents of the article.

## Funding

There is no funding to report.

## Disclosure

Non-financial competing interests. The authors report no other potential conflicts of interest for this work.

## References


1. Cohen-Rosenblum A, Cui Q. Osteonecrosis of the femoral head. *Orthop Clin North Am*. 2019;50(2):139–149. doi:10.1016/j.ocl.2018.10.001
2. Chen XJ, Shen YS, He MC, et al. Polydatin promotes the osteogenic differentiation of human bone mesenchymal stem cells by activating the BMP2-Wnt/beta-catenin signaling pathway. *Biomed Pharmacother*. 2019;112:108746. doi:10.1016/j.biopha.2019.108746
3. Zhao DW, Yu M, Hu K, et al. Prevalence of nontraumatic osteonecrosis of the femoral head and its associated risk factors in the Chinese population: results from a nationally representative survey. *Chin Med J (Engl)*. 2015;128(21):2843–2850. doi:10.4103/0366-6999.168017
4. Fu W, Liu B, Wang B, Zhao D. Early diagnosis and treatment of steroid-induced osteonecrosis of the femoral head. *Int Orthop*. 2019;43(5):1083–1087. doi:10.1007/s00264-018-4011-y
5. Baig SA, Baig MN. Osteonecrosis of the femoral head: etiology, investigations, and management. *Cureus*. 2018;10(8):e3171.
6. Lee JS, Lee JS, Roh HL, Kim CH, Jung JS, Suh KT. Alterations in the differentiation ability of mesenchymal stem cells in patients with nontraumatic osteonecrosis of the femoral head: comparative analysis according to the risk factor. *J Orthop Res*. 2006;24(4):604–609. doi:10.1002/jor.20078
7. Ruiz M, Cosenza S, Maumus M, Jorgensen C, Noel D. Therapeutic application of mesenchymal stem cells in osteoarthritis. *Expert Opin Biol Ther*. 2016;16(1):33–42. doi:10.1517/14712598.2016.1093108
8. Kriston-Pal E, Czibula A, Gyuris Z, et al. Characterization and therapeutic application of canine adipose mesenchymal stem cells to treat elbow osteoarthritis. *Can J Vet Res*. 2017;81(1):73–78.
9. Kong L, Zheng LZ, Qin L, Ho KKW. Role of mesenchymal stem cells in osteoarthritis treatment. *J Orthop Translat*. 2017;9:89–103. doi:10.1016/j.jot.2017.03.006
10. Yim RL, Lee JT, Bow CH, et al. A systematic review of the safety and efficacy of mesenchymal stem cells for disc degeneration: insights and future directions for regenerative therapeutics. *Stem Cells Dev*. 2014;23(21):2553–2567. doi:10.1089/scd.2014.0203
11. Liu Y, Wu J, Zhu Y, Han J. Therapeutic application of mesenchymal stem cells in bone and joint diseases. *Clin Exp Med*. 2014;14(1):13–24. doi:10.1007/s10238-012-0218-1
12. Sun ZB, Wang JW, Xiao H, et al. Icariin may benefit the mesenchymal stem cells of patients with steroid-associated osteonecrosis by ABCB1-promoter demethylation: a preliminary study. *Osteoporos Int*. 2015;26(1):187–197. doi:10.1007/s00198-014-2809-z
13. Houdek MT, Wyles CC, Packard BD, Terzic A, Behfar A, Sierra RJ. Decreased osteogenic activity of mesenchymal stem cells in patients with corticosteroid-induced osteonecrosis of the femoral head. *J Arthroplasty*. 2016;31(4):893–898. doi:10.1016/j.arth.2015.08.017
14. Zhang J, Zhu X, Luo F, et al. Separation and purification of neohesperidin from the albedo of Citrus reticulata cv. Suavissima by combination of macroporous resin and high-speed counter-current chromatography. *J Sep Sci*. 2012;35(1):128–136. doi:10.1002/jssc.201100695
15. Gong Y, Dong R, Gao X, et al. Neohesperidin prevents colorectal tumorigenesis by altering the gut microbiota. *Pharmacol Res*. 2019;148:104460. doi:10.1016/j.phrs.2019.104460
16. Du L, Jiang Z, Xu L, et al. Microfluidic reactor for lipase-catalyzed regioselective synthesis of neohesperidin ester derivatives and their antimicrobial activity research. *Carbohydr Res*. 2018;455:32–38. doi:10.1016/j.carres.2017.11.008
17. Lee JH, Lee SH, Kim YS, Jeong CS. Protective effects of neohesperidin and poncirin isolated from the fruits of poncirus trifoliata on potential gastric disease. *Phytother Res*. 2009;23(12):1748–1753. doi:10.1002/ptr.2840
18. Tan Z, Cheng J, Liu Q, et al. Neohesperidin suppresses osteoclast differentiation, bone resorption and ovariectomised-induced osteoporosis in mice. *Mol Cell Endocrinol*. 2017;439:369–378. doi:10.1016/j.mce.2016.09.026
19. Gupta SC, Awasthee N, Rai V, Chava S, Gunda V, Challagundla KB. Long non-coding RNAs and nuclear factor-kappaB crosstalk in cancer and other human diseases. *Biochim Biophys Acta Rev Cance*. 2019;1873(1):188316. doi:10.1016/j.bbcan.2019.188316
20. Yu F, Wang L, Zhang B. Long non-coding RNA DRHC inhibits the proliferation of cancer cells in triple negative breast cancer by down-regulating long non-coding RNA HOTAIR. *Oncol Lett*. 2019;18(4):3817–3822.
21. Wei B, Wei W, Zhao B, Guo X, Liu S. Long non-coding RNA HOTAIR inhibits miR-17-5p to regulate osteogenic differentiation and proliferation in non-traumatic osteonecrosis of femoral head. *PLoS One*. 2017;12(2):e0169097. doi:10.1371/journal.pone.0169097
22. Yan YQ, Pang QJ, Xu RJ. Effects of erythropoietin for precaution of steroid-induced femoral head necrosis in rats. *BMC Musculoskelet Disord*. 2018;19(1):282. doi:10.1186/s12891-018-2208-2
23. Fan JJ, Cao LG, Wu T, et al. The dose-effect of icariin on the proliferation and osteogenic differentiation of human bone mesenchymal stem cells. *Molecules*. 2011;16(12):10123–10133. doi:10.3390/molecules161210123
24. Fang B, Wang D, Zheng J, et al. Involvement of tumor necrosis factor alpha in steroid-associated osteonecrosis of the femoral head: friend or foe? *Stem Cell Res Ther*. 2019;10(1):5. doi:10.1186/s13287-018-1112-x
25. Livak KJ, Schmittgen TD. Analysis of relative gene expression data using real-time quantitative PCR and the 2−ΔΔCT method. *Methods*. 2001;25(4):402–408. doi:10.1006/meth.2001.1262
26. Zhai L, Sun N, Zhang B, et al. Effects of focused extracorporeal shock waves on bone marrow mesenchymal stem cells in patients with avascular necrosis of the femoral head. *Ultrasound Med Biol*. 2016;42(3):753–762. doi:10.1016/j.ultrasmedbio.2015.10.021
27. Fang B, Li Y, Chen C, et al. Huo Xue Tong Luo capsule ameliorates osteonecrosis of femoral head through inhibiting lncRNA-miat. *J Ethnopharmacol*. 2019;238:111862.
28. Ma XL, Liu ZP, Ma JX, Han C, Zang JC. Dynamic expression of Runx2, osterix and AJ18 in the femoral head of steroid-induced osteonecrosis in rats. *Orthop Surg*. 2010;2(4):278–284. doi:10.1111/j.1757-7861.2010.00100.x
29. Wang W, Liu L, Dang X, Ma S, Zhang M, Wang K. The effect of core decompression on local expression of BMP-2, PPAR-gamma and bone regeneration in the steroid-induced femoral head osteonecrosis. *BMC Musculoskelet Disord*. 2012;13(1):142. doi:10.1186/1471-2474-13-142
30. Nuttall ME, Gimble JM. Is there a therapeutic opportunity to either prevent or treat osteopenic disorders by inhibiting marrow adipogenesis? *Bone*. 2000;27(2):177–184. doi:10.1016/S8756-3282(00)00317-3
31. Zhang Q, Yang F, Chen Y, et al. Chinese herbal medicine formulas as adjuvant therapy for osteonecrosis of the femoral head: a systematic review and meta-analysis of randomized controlled trials. *Medicine (Baltimore)*. 2018;97(36):e12196. doi:10.1097/MD.0000000000012196
32. Benavente-Garcia O, Castillo J. Update on uses and properties of citrus flavonoids: new findings in anticancer, cardiovascular, and anti-inflammatory activity. *J Agric Food Chem*. 2008;56(15):6185–6205. doi:10.1021/jf8006568
33. Bing W, Pang X, Qu Q, et al. Simvastatin improves the homing of BMSCs via the PI3K/AKT/miR-9 pathway. *J Cell Mol Med*. 2016;20(5):949–961. doi:10.1111/jcmm.12795

34. Li Y, Yang F, Gao M, et al. miR-149-3p regulates the switch between adipogenic and osteogenic differentiation of BMSCs by targeting FTO. *Mol Ther Nucleic Acids*. 2019;17:590–600. doi:10.1016/j.omtn.2019.06.023
35. Wen T, Wang L, Sun XJ, Zhao X, Zhang GW, Li-Ling J. Sevoflurane preconditioning promotes activation of resident CSCs by transplanted BMSCs via miR-210 in a rat model for myocardial infarction. *Oncotarget*. 2017;8(70):114637–114647. doi:10.18632/oncotarget.23062
36. Dang X, Lian L, Wu D. The diagnostic value and pathogenetic role of lncRNA-ATB in patients with osteoarthritis. *Cell Mol Biol Lett*. 2018;23(1):55. doi:10.1186/s11658-018-0118-9
37. Peng WX, Gao CH, Huang GB. High throughput analysis to identify key gene molecules that inhibit adipogenic differentiation and promote osteogenic differentiation of human mesenchymal stem cells. *Exp Ther Med*. 2019;17(4):3021–3028.
38. Li X, Peng B, Zhu X, et al. MiR-210-3p inhibits osteogenic differentiation and promotes adipogenic differentiation correlated with Wnt signaling in ERalpha-deficient rBMSCs. *J Cell Physiol*. 2019;234(12):23475–23484. doi:10.1002/jcp.28916
39. Xiang S, Li Z, Weng X. The role of lncRNA RP11-154D6 in steroid-induced osteonecrosis of the femoral head through BMSC regulation. *J Cell Biochem*. 2019;120(10):18435–18445. doi:10.1002/jcb.29161
40. Wang Y, Feng Q, Ji C, Liu X, Li L, Luo J. RUNX3 plays an important role in mediating the BMP9-induced osteogenic differentiation of mesenchymal stem cells. *Int J Mol Med*. 2017;40(6):1991–1999.